HHS Public Access

Author manuscript

Toxicology. Author manuscript; available in PMC 2015 May 25.

Published in final edited form as:

Toxicology. 2015 March 2; 329: 80–87. doi:10.1016/j.tox.2015.01.011.

Toxicoproteomic analysis of pulmonary carbon nanotube exposure using LC-MS/MS

Gina M. Hilton[a], **Alexia J. Taylor**[a], **Christina D. McClure**[b], **Gregory N. Parsons**[b], **James C. Bonner**[a], and **Michael S. Bereman**[a,*]

[a]Department of Biological Sciences, Environmental and Molecular Toxicology, North Carolina State University, Raleigh, NC, United States

[b]Department of Chemical and Biomolecular Engineering, North Carolina State University, Raleigh, NC, United States

Abstract

Toxicoproteomics is a developing field that utilizes global proteomic methodologies to investigate the physiological response as a result of adverse toxicant exposure. The aim of this study was to compare the protein secretion profile in lung bronchoalveolar lavage fluid (BALF) from mice exposed to non-functionalized multi-walled carbon nanotubes (U-MWCNTs) or MWCNTs functionalized by nanoscale Al_2O_3 coatings (A-MWCNT) formed using atomic layer deposition (ALD). Proteins were identified using liquid chromatography tandem mass spectrometry (LC-MS/MS), and quantified using a combination of two label-free proteomic methods: spectral counting and MS1 peak area analysis. On average 465 protein groups were identified per sample and proteins were first screened using spectral counting and the Fisher's exact test to determine differentially regulated species. Significant proteins by Fisher's exact test ($p<0.05$) were then verified by integrating the intensity under the extracted ion chromatogram from a single unique peptide for each protein across all runs. A two sample *t*-test based on integrated peak intensities discovered differences in 27 proteins for control versus U-MWCNT, 13 proteins for control versus A-MWCNT, and 2 proteins for U-MWCNT versus A-MWCNT. Finally, an in-vitro binding experiment was performed yielding 4 common proteins statistically different ($p<0.05$) for both the in-vitro and in-vivo study. Several of the proteins found to be significantly different between exposed and control groups are known to play a key role in inflammatory and immune response. A comparison between the in-vitro and in-vivo CNT exposure emphasized a true biological response to CNT exposure.

Keywords

Carbon nanotube; Label-free proteomics; Pulmonary fibrosis; Toxicoproteomics

*Corresponding author at: Department of Biological Sciences, Center for Human Health and the Environment, North Carolina State University, Raleigh, NC, United States. Tel.: +1 919 515 8520. michaelbereman@ncsu.edu (M.S. Bereman).

Conflict of interest

The authors declare that there are no conflicts of interest.

Transparency document

The Transparency document associated with this article can be found in the online version.

1. Introduction

Carbon nanotubes (CNTs) have been increasingly investigated for a wide range of applications since their characterization in 1991 (Vairavapandian et al., 2008). Sumio Iijima first described CNTs as “needle-like tubes” that range from 4 to 30 nm in diameter and up to 1μm in length (Iijima, 1991). These tubes are now more commonly described as rolled sheets of hexagonal graphite, being either single-walled carbon nanotubes (SWCNTs), one layer, or multi-walled carbon nanotubes (MWCNTs), greater than one layer. CNTs have been tested and reported to be stronger than steel and a fraction of the weight (Thostenson et al., 2001), thus making them ideal for material additives (Endo et al., 2008). They are also being investigated in the medical field to serve as a targeted drug delivery vehicle, offering a larger drug pay load and greater bioavailability (Bonner, 2011). CNTs unique physical properties make them ideal for various structural support and medical applications; however, the combination of increased use of CNTs, lack of knowledge of the risks from CNT exposure (Porter et al., 2010), and the absence of proper safety requirements have all led to a greater potential for adverse occupational or environmental exposure (Maynard et al., 2004).

One of the greatest concerns over the mass production and use of CNTs is that they possess fiber-like characteristics similar to asbestos, thus creating the potential for induction of pulmonary fibrosis and lung cancer upon exposure. Several studies have shown that mice or rats exposed to CNTs by inhalation, oropharyngeal aspiration (OPA), or intratracheal instillation (IT) develop lung inflammation and pulmonary fibrosis (Bonner, 2010; Ryman-Rasmussen et al., 2009a). CNTs delivered to the lungs of mice are avidly engulfed by macrophages within the alveolar region (Lam et al., 2004) which produce a variety of soluble proteins (e.g., cytokines, growth factors, proteinases, extracellular matrix) that play roles in lung homeostasis, tissue repair, or disease pathogenesis (Mitchell et al., 2007). Additionally, the lung epithelium produces critical proteins, such as pulmonary surfactant proteins (Salvador-Morales et al., 2007) and myeloperoxidase (Klebanoff, 2005), as an innate defense immune response to foreign bodies. Fibrotic response to CNTs in the alveolar interstitium is caused by the over-production of collagen and other extracellular matrix proteins by myofibroblasts that result in an increased thickness of the connective tissue (Mercer et al., 2011). Both the fibrotic and immune responses are likely due to the generation of reactive oxygen species from residual metal content from the CNTs and the persistence of CNTs endowed by their fiberlike shape (Bonner, 2011).

A variety of post-synthesis chemical engineering modifications have been developed to enhance the unique mechanical and electronic properties of CNTs (Prato et al., 2008; Singh and Kruse 2008). Atomic layer deposition (ALD) is a novel process used to apply a highly conformal thin-film coating of oxides, metals, and hybrid metal/organic materials to CNTs to enhance conductivity, photovoltaic or catalytic applications, and attachment of biomolecules (Hyde et al., 2009; Parsons et al., 2011; Peng et al., 2007). For example, aluminum oxide (Al_2O_3) and titanium oxide change surface functionality of organic fibers, increase surface hydrophilic properties, and enhance biomolecule attachment (Parsons et al., 2011; Peng et al., 2009). Zinc oxide or titanium oxide coating imparts increased photosensitivity of CNTs for photovoltaic or catalytic applications (Peng et al., 2009). ALD

was initially developed for use in the semiconductor industry and has become increasingly used for work at the nano-scale because of the highly uniform thin film coatings that are achieved via a sequence of selflimiting reactions (George, 2010; Marichy et al., 2012; Parsons et al., 2011). ALD modified CNTs are being explored in microelectronics for enhancing conductivity, and energy storage applications (Marichy et al., 2012). In assessing the potential hazards of CNTs on human health, it is therefore important to consider CNTs that are modified by ALD.

Herein, we investigate the variations in protein secretion from mouse lungs following a 24 h acute exposure to non-functionalized or ALD-functionalized MWCNTs and control via liquid chromatography- tandem mass spectrometry (LC-MS/MS). LC-MS/MS provides a powerful platform to evaluate global changes in the proteome as a response to injury or disease. In this study, protein abundance was quantified by label-free proteomics using both spectral counts and peak intensities (Asara et al., 2008; Liao et al., 2009). Finally, we demonstrate the changes in protein expression are the result of specific biological processes through gene ontology enrichment analysis.

2. Materials and methods

Acetic acid, ammonium bicarbonate, sodium deoxycholate (SDC), dithiothreitol (DTT), iodoacetamide (IAM), formic acid (FA), ammonium hydroxide, hydrochloric acid (HCl), and bovine serum albumin (BSA) were obtained from Sigma–Aldrich (St. Louis, MO). Sequencing grade trypsin was purchased from Promega (Madison, WI). HPLC gradewater, methanol, and acetonitrile were purchased from VWR International (Morrisville, NC). The Pierce bicinchoninic acid (BCA) protein assay kit was purchased through ThermoFisher Scientific (Waltham, MA). Oasis MCX 30μm particle size solid phase extraction cartridges were obtained from Waters (Milford, MA).

2.1. Nanomaterials

MWCNT 0.5–40μm in length were synthesized by chemical vapor deposition and purchased from Helix Materials Solutions (Richardson, TX). Characterization of the MWCNTs was provided by the manufacturer and verified by Millennium Research Laboratories (Woburn, MA) (Ryman-Rasmussen et al., 2009b). MWCNTs were surface coated with Al_2O_3 via atomic layer deposition (ALD). The aluminum oxide layer is achieved using sequential saturation exposures of trimethylaluminum ($Al(CH_3)_3$) and water, then separated by inert gas purging steps. Based on the known growth rate for the Al_2O_3 ALD process on MWCNTs, the nanotubes used in this study had a coating estimated to be ~50 ALD layers (Fig. 1). The details of ALD coating of carbon nanotubes have been previously described (Devine et al., 2011).

2.2. Preparation of MWCNTs

Uncoated MWCNTs (U-MWCNT) and aluminum oxide coated (A-MWCNT) were weighed using a milligram scale (Mettler, Toledo, OH) suspended in a sterile, 0.1% pluronic F-68 (Sigma–Aldrich, St. Louis, MO) in phosphate buffer solution to achieve the final concentration of 10 mg/mL. Vials containing the suspended nanomaterials were dispersed

using a cuphorn sonicator (Qsonica, Newton CT) at room temperature for 1 min prior to dosing. A limulus amebocyte lysate (LAL) chromogenic assay (Lonza Inc., Walkersville, MD) was used to test the nanomaterials for endotoxin contamination. All MWCNTs, both U-MWCNT and A-MWCNT, tested negative (<0.3 EU/mL) for endotoxin.

2.3. Exposure of mice to MWCNTs and processing of lung tissue

Mice (C57BL6, Jackson Laboratories) approximately 6–8 weeks old were exposed to U-MWCNT and A-MWCNT at 4 mg/kg in 0.1% pluronic surfactant solution or 0.1% pluronic alone for control, via oropharyngeal aspiration while under isoflurane anesthesia. Three mice per group were evaluated. Mice were euthanized via intraperitoneal injection of Fatal Plus (Vortech Pharmaceuticals, Dearborn, MI) on day 1 after MWCNT exposure (Bonner et al., 2013). At necropsy, the lungs were serially lavaged two times with 0.5 ml Dulbecco's Phosphate Buffered Saline and bronchoalveolar lavage fluids (BALFs) were collected. Lung lavages were centrifuged at 14,000 rpm for 2 min, and isolated away from MWCNTs.

2.4. In solution protein digestion

Samples were quantified by a BCA protein assay, and a final concentration of 50mM total ammonium bicarbonate (pH 8.0) was achieved by adding the appropriate amount of ammonium bicarbonate solution to the BALFs. SDC was added to generate a final concentration of 1% detergent. Disulfides were reduced upon addition of 5mM DTT and incubated for 30min at 60 °C. Samples were then cooled to room temperature and IAM was added to make a final concentration of 15mM, and incubated in the dark for 20min at room temperature. Tryptic digestion was achieved by hydrating lyophilized trypsin to a stock solution of 1μg/μL with 0.01% acetic acid in water. The trypsin solution was added to the protein mixture (i.e. 20μg protein) in a 1:50 ratio (~0.4μg trypsin), and then incubated at 37 °C for 4 h. Following the digestion, samples were acidified with 6M HCl to make a final concentration of 250mM (pH ≤ 3) (Bereman et al., 2012). Sample purification and concentration was achieved using MCX cartridges. Samples were added to the conditioned column after steps1–4(SupplementalTable1). After the sample was added to the column, salts were removed with water (0.1% formic acid), neutrals and negatively charged species were removedwith1mLofmethanol (0.1%formic acid), andthenpeptides were eluted in 10% NH_4OH in methanol. Finally, samples were concentrated down in vacuo (10 Torr) at 45 °C for 2 h (speedvac concentrator, Thermo Fisher Scientific), and then reconstituted in mobile phase A (98% water, 2% acetonitrile, and 0.1% formic acid) to yield a final concentration 100 ng/μL.

2.5. In-vivo exposure of mouse lung lavage to MWCNTs

Each of the 9 lung lavage samples (3 controls, 3 U-MWCNT exposures, and 3 A-MWCNT exposures) were isolated from mice as described in the 'Exposure of mice to MWCNTs and processing of lung tissue', and then diluted to 175μL with 50mM ammonium bicarbonate solution. Sample digestion and purification was achieved as described in the 'In solution protein digestion' section. A final sample concentrationwas 100 ng/μL peptide was prepared for LC-MS/MS.

2.6. *In-vitro* exposure of mouse lung lavage to MWCNTs

A single lung lavage sample from a control mouse (C57BL6, Jackson Laboratories)was isolated, as described in the 'Exposure of mice to MWCNTs and processing of lung tissue.', and divided into 3 separate aliquots. The sample was quantified and recorded to be 0.2μg/μL protein concentration. Each aliquot contained 150μL of 0.1% pluronic solution to yield 30μg of protein. The designated U- and A-MWCNT samples received 4 mg/kg of respective MWCNTs in 0.1% pluronic surfactant solution, and the control received 0.1% pluronic alone to ensure equal concentrations. Samples were incubated and shaken for 24 h at 37 °C and 180 rpm (MaxQ 4000, Thermo Fisher Scientific). After incubation, samples were centrifuged at 14,000 rpm for 2 min, and isolated away from MWCNTs. Lung lavages were further diluted with 400mM ammonium bicarbonate to achieve a final concentration of 50mM in 200μL total volume. Each sample pH was checked and recorded to be 8.0. Sample digestion was achieved as described in the 'In solution protein digestion' section. A final sample concentration of 0.5μg/μL peptide was prepared for LC-MS/MS.

2.7. LC-MS/MS

Nanoflow liquid chromatography (LC) was conducted using the Thermo Scientific Easy-nLC 1000 Liquid Chromatography system. Pico-Frit columns were purchased from New Objective (Woburn, MA) and packed to a length of 20cm with reverse phase ReproSil-Pur 120C-18-AQ 3μm particles (Dr. Maisch, Germany). The trap was packed in house to a final length of 3 cm. A 2μL injection (200 ng total protein) was washed onto the trap at a flow of 2.0 μL/min for 4 min. Peptide separationwas achieved on the LC using a gradient of mobile phase A (98% water, 2% acetonitrile, and 0.1% formic acid) and mobile phase B (100% acetonitrile, 0.1% formic acid). The 90 min method consisted of an LC gradient with a linear ramp from 2% B to 40% B across 70 min (2–72 min), a ramp and wash at 80% B (72–78 min), followed by equilibration of the column at 0% B (Supplemental Table 2). Tandem mass spectrometry was performed using a Thermo Scientific Q-Exactive Plus in a top 12 mode where the 12 most abundant precursors were selected for fragmentation per full scan. MS1 and MS2 scans were performed at a resolving power of 70 k and 17.5 k at *m*/*z* 200, respectively. A dynamic exclusion window of 30 s was used to avoid repeated interrogation of abundant species. Automatic gain control was 1e6 and 5e4 for MS1 and MS2 scans, respectively. A quality control BSA digest was run every fifth injection to ensure proper LC-MS/MS reproducibility. Metrics were monitored in using the Statistical Process Control in Proteomics algorithm (Bereman et al., 2014).

2.8. Database search

Database searches were conducted using Proteome Discoverer 1.4 and the Sequest hyper-threaded algorithm. Data were searched against the *Mus musculus* Swiss Prot protein database (number of sequences: 16,657, date accessed: 02/11/2014) (UniProt, 2008). Peptide spectrum matches were post processed using percolator to enforce a peptide spectral match threshold of q-value<0.01. The law of strict parsimony was used for protein inference and grouping (Zhang et al., 2007).

2.9. Data analysis

The experimental data were exported from Proteome Discoverer as an inclusive tab delimited file containing each protein group ID and spectral count. A protein's spectral count is the total sum of the number of times peptides belonging to that protein were identified in the experiment. It is a fast method for relative quantification and identification of putative proteins of interest (Liu et al., 2004). Missing spectral count data for any protein group (i.e., not identified) was assigned a zero. Each experimental group's spectral count data was summed by protein group ID to generate 3 groups of 3 samples each: control, U-MWCNT, and A-MWCNT. We first screened the list of proteins identified using the Fisher's exact test to calculate *p*-values based on the combined spectral count of each protein for each pairwise comparison: control versus U-MWCNT, control versus A-MWCNT, and U-MWCNT versus A-MWCNT. Next, these results were further verified by integrating the summed area under the extracted ion chromatogram of the M, M+ 1, and M+ 2 signals of a single unique peptide from each putative protein of interest identified from the Fisher's exact test using MS1 full scan filtering in Skyline (MacLean et al., 2010; Schilling et al., 2012). Spectral libraries were created directly in Skyline from the .msf files and used in combination with mass measurement accuracy, retention time reproducibility, and isotope dot products to integrate signals corresponding to peptides of interest. Unique peptides for each protein were determined using the background proteome database function in Skyline. The peak area data were log transformed, all zero values were imputed with a value of 10, and *p*-values were calculated by using a two-sample *t*-test for each group (Supplemental Table 3). Proteins that were identified as significant by both spectral count ($p<0.05$) and peak intensity integration ($p<0.05$) were further analyzed by gene ontology enrichment analysis using the DAVID Bioinformatics Resources 6.7 database (Huang da et al., 2009).

In-vitro experimental data was processed similarly to the in-vivo experimental data, as described above. Analytical replicate spectral count datawas summed for each of the 3 samples: control, U-MWCNT, and A-MWCNT. Fisher's exact test was run for each pairwise comparison.

3. Results

3.1. In-vivo study

The experimental design for in-vivo mouse exposure to A-MWCNT and U-MWCNT, followed by lung lavage isolation, protein digestion, LC-MS/MS, and data analysis is shown in Fig. 2. Fig. 3displays volcano plots in which the $\log_2$ fold change is plotted against $-\log_{10}$ *p*-value generated from the Fisher's exact test. Of the protein groups identified by SEQUEST across the sample set, 68 were significantly different by the Fisher's exact test (*p*-value <0.05) in control versus U-MWCNT, 47 significant by control versus A-MWCNT, and 21 significant by U- versus A-MWCNT. Thus, a greater than 2 fold difference in number of protein groups significant by Fisher's exact test were detected between the control and each MWCNT-exposed group versus the differences between the both of the exposed groups. Further examination of the significant proteins identified by spectral counting between the control and U-MWCNT groups were investigated by MS1 peak area analysis in Skyline. A total of 26 proteins found to be significant by the Fisher's exact test

across all combinations of comparison did not have a unique peptide that could be confidently integrated using the rules outlined in the methods section due largely to low signal to noise, and thus were not included in the analysis of the comparisons. Fig. 4illustrates an example of peak area analysis and subsequent *t*-test results for myeloperoxidase. Of the significant proteins found by Fisher's exact test that were further analyzed by peak area analysis, 27 proteins were found to be significant (p-value<0.05) between control versus U-MWCNT, 13 proteins were significant between control versus A-MWCNT, and 2 proteins were significant between U-MWCNT versus A-MWCNT (Supplemental Table 3). These results illustrate the more conservative p-value by peptide peak area analysis compared to spectral counting, which is attributed to a combination of accounting for the variance amongst the biological replicates inherent in the *t*-statistic, raw spectral counts include possible non-unique peptides, and not every protein had a unique peptide that could be confidently integrated. Fig. 4A illustrates peak area analysis of myeloperoxidase, a protein associated with innate immune response, where the protein was not detected in the control, but was detected in both of the exposed groups. Myeloperoxidase levels across control and exposed groups were not significant in the in-vitro study, and therefore, are more likely to be a true biological response versus a physical interaction of the MWCNTs adhering to the protein.

3.2. *In-vitro* study

To confirm a true biological response, as opposed to a physical interaction, we conducted an in-vitro study to probe for potential protein binding with MWCNTs. Of the approximately 500 proteins groups identified, 11 proteins were statistically significant by Fisher's exact test (p-value<0.05) for control versus U-MWCNT, and 15 proteins for the control versus A-MWCNT as illustrated in the volcano plot in Supplemental Fig. 1. However, only 4 proteins were identified as significant by the Fisher's exact test in both the in-vitro and in-vivo study. These results indicate that the remaining proteins identified as being statistically significant in the in-vivo study are due to a true biological response and not physical binding of MWCNTs to proteins.

3.3. Gene ontology analysis

Gene ontology (GO) enrichment analysis was used to further classify the biological function of the significant proteins calculated by *t*-test for the control versus U-MWCNT, and the control versus A-MWCNT in the in-vivo study. Fig. 5illustrates the GO analysis results for both biological process and molecular function. Biological processes are (1) considered molecular events with a beginning and end, and (2) have a vital role in living units (i.e. cells, tissues, organs, and organisms). Molecular function GO term defines the functions of gene products in accordance with their abilities. Of the biological process GO terms identified in the comparison of control versus U-MWCNT, 58% were identified in the category of response to stimulus, and the remaining 42% were identified in the category of immune response (Supplemental Table 4). The significant biological process GO terms identified the control versus A-MWCNT comparison comprised 75% related to a response to stimulus, and 25% an immune response. The results of the GO analysis for the control versus MWCNT exposed groups show enrichment for proteins in both immune response, and response to stimuli.

4. Discussion

The aim of this study was to investigate proteomic changes upon acute pulmonary exposure to coated and uncoated MWCNTs. Of the proteins that were found to be statistically significant by comparing control versus MWCNT exposed groups, several were identified to be associated with an immune response and/or a response to stimuli, including: myeloperoxidase (MPO), lacto-transferrin (LTF), neutrophil gelatinase-associated lipocalin (NGAL), histone H4, pulmonary surfactant-associated protein B (SP-B), and complement (C3, C4b, and C9) proteins. It has been well established that neutrophils use MPO, a lysosomal enzyme, as an innate immune response to kill microbes by generating hydrogen peroxide (Gaut et al., 2001; Klebanoff, 2005). In this study we observed significantly increased levels of MPO expression in both of the exposed groups and no detectable expression in the control, thus indicating a pulmonary immune response to injury upon MWCNT exposure. Interestingly, MPO has recently been shown to degrade MWCNTs and therefore MPO represents a potentially important defense to break down otherwise persistent nanotubes (Kagan et al., 2010). Moreover, mice deficient in MPO had reduced clearance of CNTs and enhanced inflammation and fibrosis (Shvedova et al., 2012). Our data show that uncoated and Al_2O_3-coated MWCNT both induce MPO protein expression equally in the lungs of mice. However, it is possible that the Al_2O_3 coating might alter MPO-induced degradation of CNTs and this is an important issue to address in future studies.

In addition to MPO, LTF, also known as lactoferrin, is present in neutrophil granules and plays an important role to bridge the innate and adaptive immune response by aiding cellular regulation of oxidative stress, as well as, control excess inflammatory response (Actor et al., 2009). Like MPO, LTF protein expression was also significantly increased upon both U-MWCNT and A-MWCNT exposure which indicates an up regulated process to control for inflammatory response in the lung. Additional evidence of innate immune response and inflammatory induction by MWCNT exposure was found by the increased expression of NGAL in both U-MWCNT and A-MWCNT exposure compared to the control, and an increase in histone H4 in the U-MWCNT exposed groups compared to control. NGAL is known to be expressed by immune cells and serves to modulate oxidative stress, and when reactive oxygen species are generated upon exposure, DNA damage can occur and release histone H4 and serve as a marker for inflammatory response (Chakraborty et al., 2012; Tambor et al., 2013). Along with NGAL and histone H4, immune defense systems, such as the complement component system, have been detected for up regulation upon MWCNT exposure. The complement system, containing more than 30 proteins, is considered to play a vital role in innate immune response, and can be activated through three major pathways: classical, lectin, and alternative (Dunkelberger and Song, 2010). Initiation of the classical pathway occurs through antigen/antibody immune complexes, the lectin pathway occurs by lectins recognition of pathogen-associated molecular patterns (PAMPs), and the alternative pathway is activated by interaction with pathogenic surfaces. Our data analysis showed statistically significant differences in complement components C9, C3, and C4b in the U-MWCNT exposed group compared to the control. C9 is a part of the terminal complement component system that serves to initiate membrane attack on certain pathogens and cells. C3 protein acts through the alternative pathway and is broken down by C3 convertase to C3b, a

protein that binds complement receptors on phagocytes, and C3a, a mediator of inflammation. Lastly, C4b acts as an opsonin on the surface of targeted cells. All three complement components were up regulated in U-MWCNT exposure compared to the control, thus indicating activation of the complement component system as an innate immune response.

Another key protein group known to induce immune response are the pulmonary surfactant proteins (SP), including: SP-A, SP-B, and SP-D. Surfactant proteins compose a major component of pulmonary surfactant which is essential for maintaining lung homeostasis as it prevents alveolar collapse (Wright, 2005). Induction of immune response has been shown to be enhanced by SP-B containing antigen vesicles within the airways (van Iwaarden et al., 2001). Our proteomic analysis demonstrated that of the 3 common surfactant proteins, only SP-B was statistically significant in the comparison of U-MWCNT versus control. Interestingly, SP-B was detected in lower levels for both of the exposed groups compared to the control, thus following the trend previously observed with SP-A and SP-D where the proteins were bound to the CNTs (Salvador-Morales et al., 2007). The reduction in SP-B levels could be indicative of an immune response whereby the secreted proteins are adhering to the CNTs. However, none of the surfactant proteins were significant by the in-vitro study, indicating that the binding of the surfactant proteins to the CNTs may be concentration and/or environment dependent.

Comparing the different MWCNT (Al_2O_3-coated versus uncoated) exposure groups yielded little differences in protein abundances, thus indicating the major response in this specific study was due to CNT exposure. However, more precise absolute quantitative LC-MS/MS methods are needed to screen a variety of different coatings based on the markers identified herein and will be the subject of future studies.

5. Conclusion

This study examined changes in protein abundance associated with immune response and inflammation were detected in mice lung BALF after 24 h exposure to functionalized and non-functionalized MWCNTs. These experiments demonstrated the ability to use LC-MS/MS to probe for global changes in lung lavage fluid upon pulmonary insult to carbon nanotubes. Differences in protein expression were screened by examining spectral count data and further verified by peak area analysis of a single unique peptide. Investigation of the potential protein interaction with CNTs was conducted as an in-vitro study to examine whether biological changes in protein expression occur upon toxicant exposure versus protein binding with the CNTs. Further protein binding studies are needed to examine potential protein interaction with various functionalized CNTs. Future studies will use protein cleavage isotope dilution mass spectrometry to validate the absolute changes in protein amounts and examine the differences in protein expression across multiple types of MWCNT functionalization. In addition, we will use global proteomic approaches to investigate perturbations of intracellular pathways in relation to carbon nanotube functionalization using model cell lines. Ultimately, putative markers of interest will be used to develop targeted peptide assays based on selected reaction monitoring to determine degree of toxicity of a variety of carbon nanotube coatings.

Supplementary Material

Refer to Web version on PubMed Central for supplementary material.

Acknowledgment

The authors acknowledge support from the NIEHS Training Grant: Molecular Pathways to Pathogenesis in Toxicology T32 ES007046, the NIEHS R01ES020897, and the NIEHS RC2ES018772.

Abbreviations

Al_2O_3	aluminum oxide
A-MWCNT	aluminum oxide-coated multi-walled carbon nanotubes
ALD	atomic layer deposition
BCA	bicinchoninic acid
BSA	bovine serum albumin
BALF	bronchoalveolar lavage fluid
CNTs	carbon nanotubes
C3, C4b, and C9	complement system proteins
DTT	dithiothreitol
FA	formic acid
GO	gene ontology
HPLC	high-performance liquid chromatography
HCl	hydrochloric acid
IT	intratracheal instillation
IAM	iodoacetamide
LTF	lactotransferrin
LC-MS/MS	liquid chromatography tandem mass spectrometry
MWCNT	multi-walled carbon nanotubes
MPO	myeloperoxidase
NGAL	neutrophil gelatinase-associated lipocalin
OPA	oropharyngeal aspiration
SP-A, B, D	pulmonary surfactant-associated protein
SWCNT	single-walled carbon nanotubes
SDC	sodium deoxycholate
U-MWCNT	un-coated multi-walled carbon nanotubes

Appendix A. Supplementary data

Supplementary data associated with this article can be found, in the online version, at http://dx.doi.org/10.1016/j.tox.2015.01.011.

References

Actor JK, Hwang SA, Kruzel ML. Lactoferrin as a natural immune modulator. Curr. Pharm. Des. 2009; 15:1956–1973. [PubMed: 19519436]

Asara JM, Christofk HR, Freimark LM, Cantley LC. A label-free quantification method by MS/MS TIC compared to SILAC and spectral counting in a proteomics screen. Proteomics. 2008; 8:994–999. [PubMed: 18324724]

Bereman MS, Canterbury JD, Egertson JD, Horner J, Remes PM, Schwartz J, Zabrouskov V, MacCoss MJ. Evaluation of front-end higher energy collision-induced dissociation on a benchtop dual-pressure linear ion trap mass spectrometer for shotgun proteomics. Anal. Chem. 2012; 84:1533–1539. [PubMed: 22192247]

Bereman MS, Johnson R, Bollinger J, Boss Y, Shulman N, MacLean B, Hoofnagle AN, MacCoss MJ. Implementation of statistical process control for proteomic experiments via LC MS/MS. J. Am. Soc. Mass Spectrom. 2014; 25:581–587. [PubMed: 24496601]

Bonner JC. Nanoparticles as a potential cause of pleural and interstitial lung disease. Proc. Am. Thoracic Soc. 2010; 7:138–141.

Bonner JC. Carbon nanotubes as delivery systems for respiratory disease: do the dangers outweigh the potential benefits? Expert Rev. Respir. Med. 2011; 5:779–787. [PubMed: 22082164]

Bonner JC, Silva RM, Taylor AJ, Brown JM, Hilderbrand SC, Castranova V, Porter D, Elder A, Oberdorster G, Harkema JR, Bramble LA, Kavanagh TJ, Botta D, Nel A, Pinkerton KE. Interlaboratory evaluation of rodent pulmonary responses to engineered nanomaterials: the NIEHS Nano GO Consortium. Environ. Health Perspect. 2013; 121:676–682. [PubMed: 23649427]

Chakraborty S, Kaur S, Guha S, Batra SK. The multifaceted roles of neutrophil gelatinase associated lipocalin (NGAL) in inflammation and cancer. Biochim. Biophys. Acta. 2012; 1826:129–169. [PubMed: 22513004]

Devine CK, Oldham CJ, Jur JS, Gong B, Parsons GN. Fiber containment for improved laboratory handling and uniform nanocoating of milligram quantities of carbon nanotubes by atomic layer deposition. Langmuir. 2011; 27:14497–14507. [PubMed: 22070742]

Dunkelberger JR, Song WC. Complement and its role in innate and adaptive immune responses. Cell Res. 2010; 20:34–50. [PubMed: 20010915]

Endo M, Strano MS, Ajayan PM. Potential applications of carbon nanotubes. Carbon Nanotubes. 2008; 111:13–61.

Gaut JP, Yeh GC, Tran HD, Byun J, Henderson JP, Richter GM, Brennan ML, Lusis AJ, Belaaouaj A, Hotchkiss RS, Heinecke JW. Neutrophils employ themyeloperoxidase system to generate antimicrobial brominating and chlorinating oxidants during sepsis. Proc. Natl. Acad. Sci. U. S. A. 2001; 98:11961–11966. [PubMed: 11593004]

George SM. Atomic layer deposition: an overview. Chem. Rev. 2010; 110:111–131. [PubMed: 19947596]

Huang da W, Sherman BT, Lempicki RA. Systematic and integrative analysis of large gene lists using DAVID bioinformatics resources. Nat. Protoc. 2009; 4:44–57. [PubMed: 19131956]

Hyde GK, McCullen SD, Jeon S, Stewart SM, Jeon H, Loboa EG, Parsons GN. Atomic layer deposition and biocompatibility of titanium nitride nanocoatings on cellulose fiber substrates. Biomed. Mater. 2009; 4:25001.

Iijima S. Helical microtubules of graphitic carbon. Nature. 1991; 354:56–58.

Kagan VE, Konduru NV, Feng W, Allen BL, Conroy J, Volkov Y, Vlasova II, Belikova NA, Yanamala N, Kapralov A, Tyurina YY, Shi J, Kisin ER, Murray AR, Franks J, Stolz D, Gou P, Klein-Seetharaman J, Fadeel B, Star A, Shvedova AA. Carbon nanotubes degraded by neutrophil

myeloperoxidase induce less pulmonary inflammation. Nat. Nanotechnol. 2010; 5:354–359. [PubMed: 20364135]

Klebanoff SJ. Myeloperoxidase: friend and foe. J. Leukoc. Biol. 2005; 77:598–625. [PubMed: 15689384]

Lam CW, James JT, McCluskey R, Hunter RL. Pulmonary toxicity of single-wall carbon nanotubes in mice 7 and 90 days after intratracheal instillation. Toxicol. Sci. 2004; 77:126–134. [PubMed: 14514958]

Liao L, McClatchy DB, Yates JR. Shotgun proteomics in neuroscience. Neuron. 2009; 63:12–26. [PubMed: 19607789]

Liu H, Sadygov RG, Yates JR. A model for random sampling and estimation of relative protein abundance in shotgun proteomics. Anal. Chem. 2004; 76:4193–4201. [PubMed: 15253663]

MacLean B, Tomazela DM, Shulman N, Chambers M, Finney GL, Frewen B, Kern R, Tabb DL, Liebler DC, MacCoss MJ. Skyline: an open source document editor for creating and analyzing targeted proteomics experiments. Bioinformatics. 2010; 26:966–968. [PubMed: 20147306]

Marichy C, Bechelany M, Pinna N. Atomic layer deposition of nanostructured materials for energy and environmental applications. Adv. Mater. 2012; 24:1017–1032. [PubMed: 22278762]

Maynard AD, Baron PA, Foley M, Shvedova AA, Kisin ER, Castranova V. Exposure to carbon nanotube material: aerosol release during the handling of unrefined single-walled carbon nanotube material. J. Toxicol. Environ. Health A. 2004; 67:87–107. [PubMed: 14668113]

Mercer RR, Hubbs AF, Scabilloni JF, Wang L, Battelli LA, Friend S, Castranova V, Porter DW. Pulmonary fibrotic response to aspiration of multi-walled carbon nanotubes. Part. Fibre Toxicol. 2011; 8:21. [PubMed: 21781304]

Mitchell LA, Gao J, Wal RV, Gigliotti A, Burchiel SW, McDonald JD. Pulmonary and systemic immune response to inhaled multiwalled carbon nanotubes. Toxicol. Sci. 2007; 100:203–214. [PubMed: 17660506]

Parsons GN, George SM, Knez M. Progress and future directions for atomic layer deposition and ALD-based chemistry. MRS Bull. 2011; 36:865–871.

Peng Q, Gong B, VanGundy RM, Parsons GN. Zincone zinc oxide-organic hybrid polymer thin films formed by molecular layer deposition. Chem. Mater. 2009; 21:820–830.

Peng Q, Sun XY, Spagnola JC, Hyde GK, Spontak RJ, Parsons GN. Atomic layer deposition on electrospun polymer fibers as a direct route to AL2O3 microtubes with precise wall thickness control. Nano Lett. 2007; 7:719–722. [PubMed: 17279801]

Porter DW, Hubbs AF, Mercer RR, Wu N, Wolfarth MG, Sriram K, Leonard S, Battelli L, Schwegler-Berry D, Friend S, Andrew M, Chen BT, Tsuruoka S, Endo M, Castranova V. Mouse pulmonary dose- and time course-responses induced by exposure to multi-walled carbon nanotubes. Toxicology. 2010; 269:136–147. [PubMed: 19857541]

Prato M, Kostarelos K, Bianco A. Functionalized carbon nanotubes in drug design and discovery. Acc. Chem. Res. 2008; 41:60–68. [PubMed: 17867649]

Ryman-Rasmussen JP, Cesta MF, Brody AR, Shipley-Phillips JK, Everitt JI, Tewksbury EW, Moss OR, Wong BA, Dodd DE, Andersen ME, Bonner JC. Inhaled carbon nanotubes reach the subpleural tissue in mice. Nat. Nanotechnol. 2009a; 4:747–751. [PubMed: 19893520]

Ryman-Rasmussen JP, Tewksbury EW, Moss OR, Cesta MF, Wong BA, Bonner JC. Inhaled multiwalled carbon nanotubes potentiate airway fibrosis in murine allergic asthma. Am. J. Respir. Cell Mol. Biol. 2009b; 40:349–358. [PubMed: 18787175]

Salvador-Morales C, Townsend P, Flahaut E, Venien-Bryan C, Vlandas A, Green MLH, Sim RB. Binding of pulmonary surfactant proteins to carbon nanotubes; potential for damage to lung immune defense mechanisms. Carbon. 2007; 45:607–617.

Schilling B, Rardin MJ, MacLean BX, Zawadzka AM, Frewen BE, Cusack MP, Sorensen DJ, Bereman MS, Jing E, Wu CC, Verdin E, Kahn CR, Maccoss MJ, Gibson BW. Platform-independent and label-free quantitation of proteomic data using MS1 extracted ion chromatograms in skyline: application to protein acetylation and phosphorylation. Mol. Cell. Proteomics. 2012; 11:202–214. [PubMed: 22454539]

Shvedova AA, Kapralov AA, Feng WH, Kisin ER, Murray AR, Mercer RR, St Croix CM, Lang MA, Watkins SC, Konduru NV, Allen BL, Conroy J, Kotchey GP, Mohamed BM, Meade AD, Volkov

Y, Star A, Fadeel B, Kagan VE. Impaired clearance and enhanced pulmonary inflammatory/fibrotic response to carbon nanotubes in myeloperoxidase-deficient mice. PloS One. 2012; 7:e30923. [PubMed: 22479306]

Singh S, Kruse P. Carbon nanotube surface science. Int. J. Nanotechnol. 2008; 5:900.

Tambor V, Kacerovsky M, Lenco J, Bhat G, Menon R. Proteomics and bioinformatics analysis reveal underlying pathways of infection associated histologic chorioamnionitis in pPROM. Placenta. 2013; 34:155–161. [PubMed: 23246098]

Thostenson ET, Ren ZF, Chou TW. Advances in the science and technology of carbon nanotubes and their composites: a review. Compos. Sci. Technol. 2001; 61:1899–1912.

UniProt C. The universal protein resource (UniProt). Nucleic Acids Res. 2008; 36:D190–D195. [PubMed: 18045787]

Vairavapandian D, Vichchulada P, Lay MD. Preparation and modification of carbon nanotubes: review of recent advances and applications in catalysis and sensing. Anal. Chim. Acta. 2008; 626:119–129. [PubMed: 18790113]

van Iwaarden JF, Claassen E, Jeurissen SH, Haagsman HP, Kraal G. Alveolar macrophages, surfactant lipids, and surfactant protein B regulate the induction of immune responses via the airways. Am. J. Respir. Cell Mol. Biol. 2001; 24:452–458. [PubMed: 11306439]

Wright JR. Immunoregulatory functions of surfactant proteins. Nat. Rev. Immunol. 2005; 5:58–68. [PubMed: 15630429]

Zhang B, Chambers MC, Tabb DL. Proteomic parsimony through bipartite graph analysis improves accuracy and transparency. J. Proteome Res. 2007; 6:3549–3557. [PubMed: 17676885]

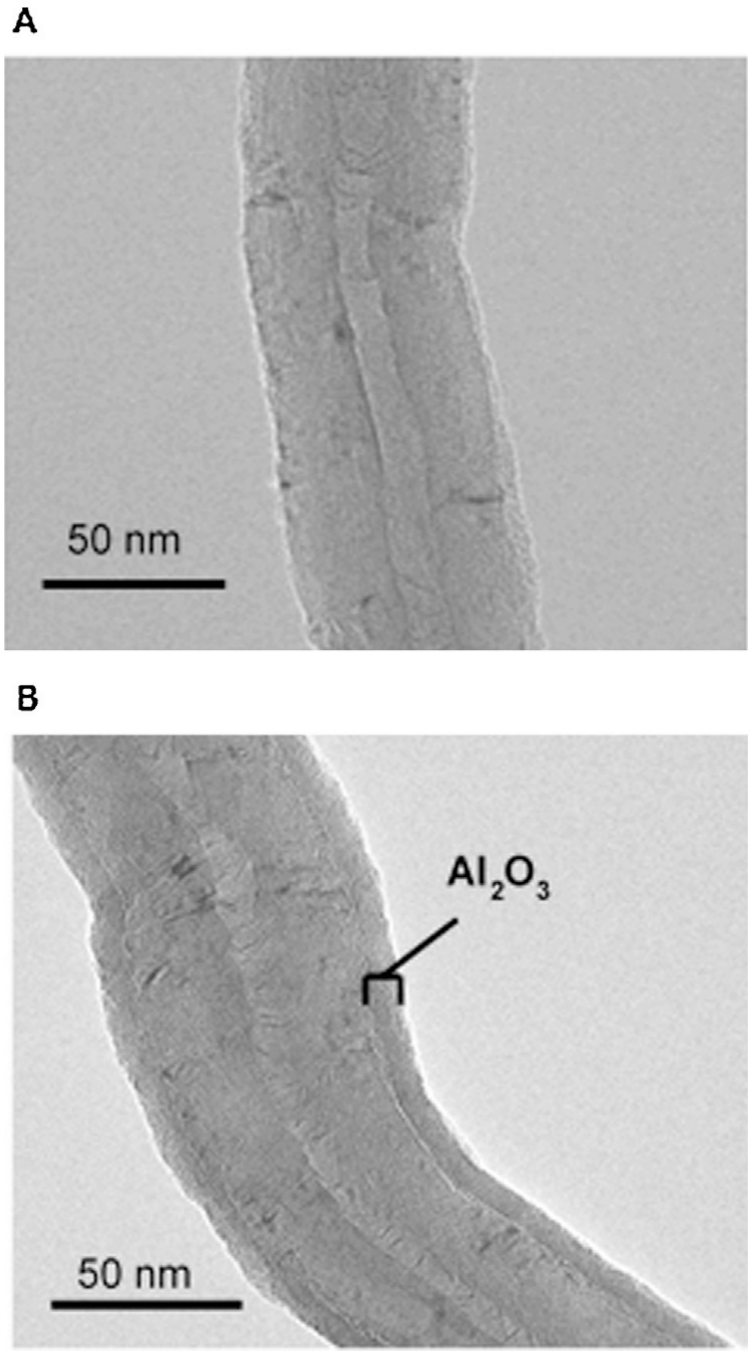

Fig. 1.

Transmission electron photomicrographs of (A) non-functionalized MWCNTs and (B) ALD Al_2O_3-functionalized MWCNTs.

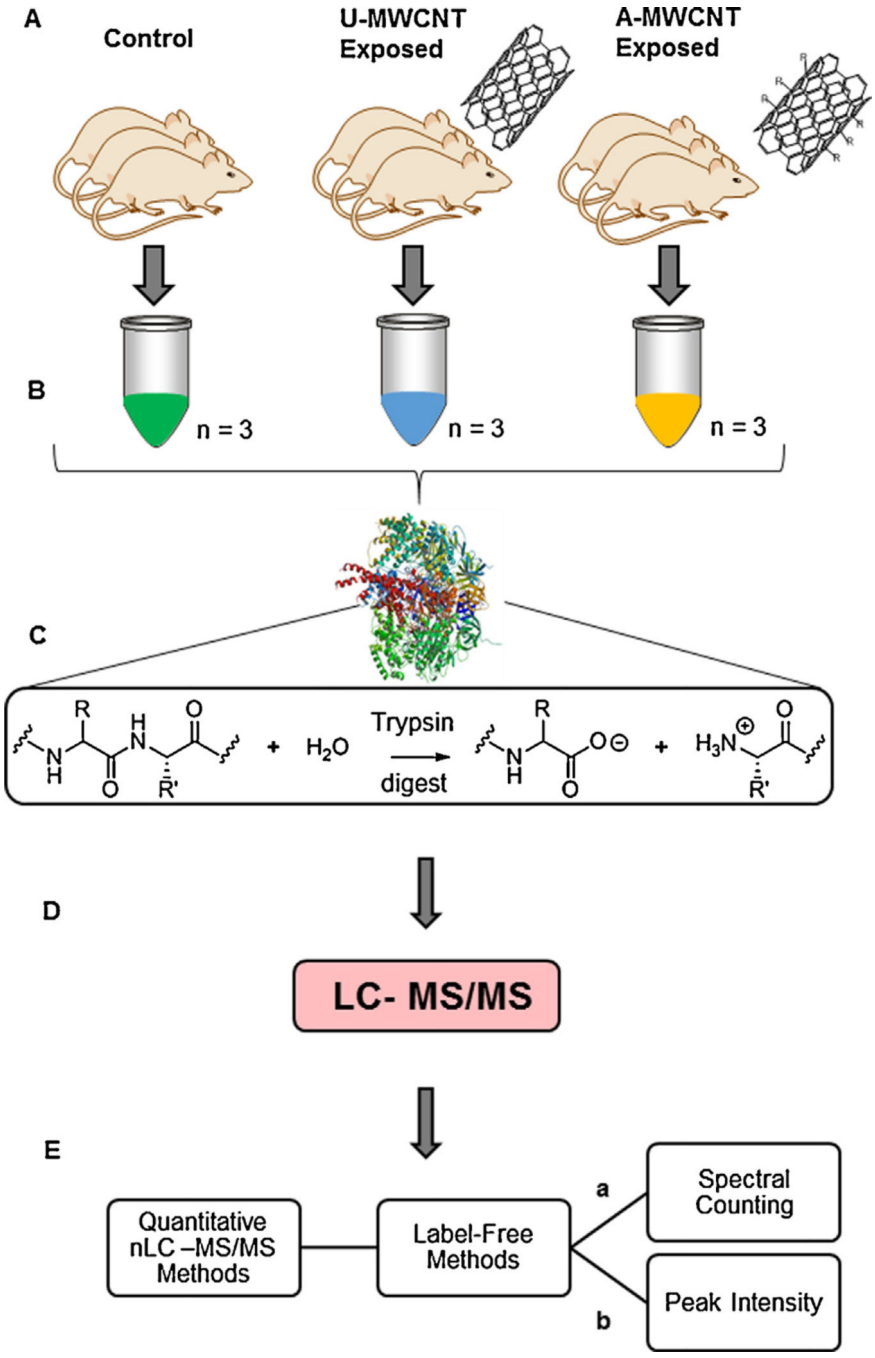

Fig. 2.

General overview of sample preparation and data analysis. (A) Mouse exposure toMWCNTs, (B) lung lavage extraction, (C) tryptic digestion of lung lavage and SPE sample clean up, (D) LC-MS/MS, and (E) Label-free protein quantification by: (a) spectral counting, and (b) verification by MS1 peak area analysis of unique peptides.

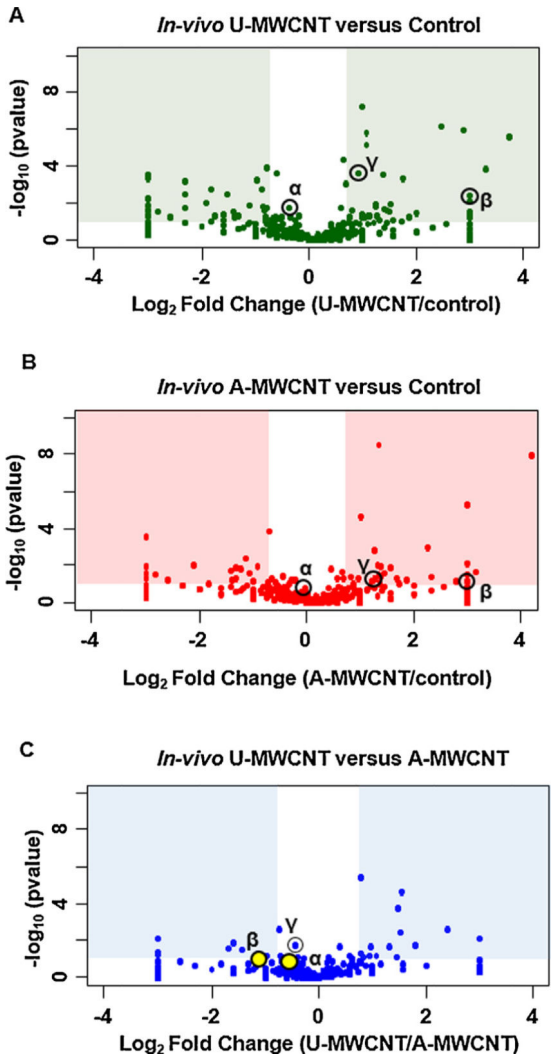

Fig. 3.

Volcano plots of $\log_2$ spectral count fold change versus-$\log_{10}$ *p*-value calculated by Fisher's exact test for: (A) U-MWCNT/control, (B) A-MWCNT/control, and (C) U-MWCNT/A-MWCNT. Proteins plotted as a log2 fold change of 3 and -3 represent protein detection in exposed groups, but not control, and vice versa (respectively). Positive fold change in spectral count data represent up-regulation in exposed groups versus the control. Shaded areas highlight significance of $p<0.05$. Abundant proteins (i.e., human serum albumin) were included in calculations of the Fisher's exact test, but not shown in plots. α = Pulmonary surfactant-associated protein-B. β =Myeloperoxidase. γ = Lactotransferrin.

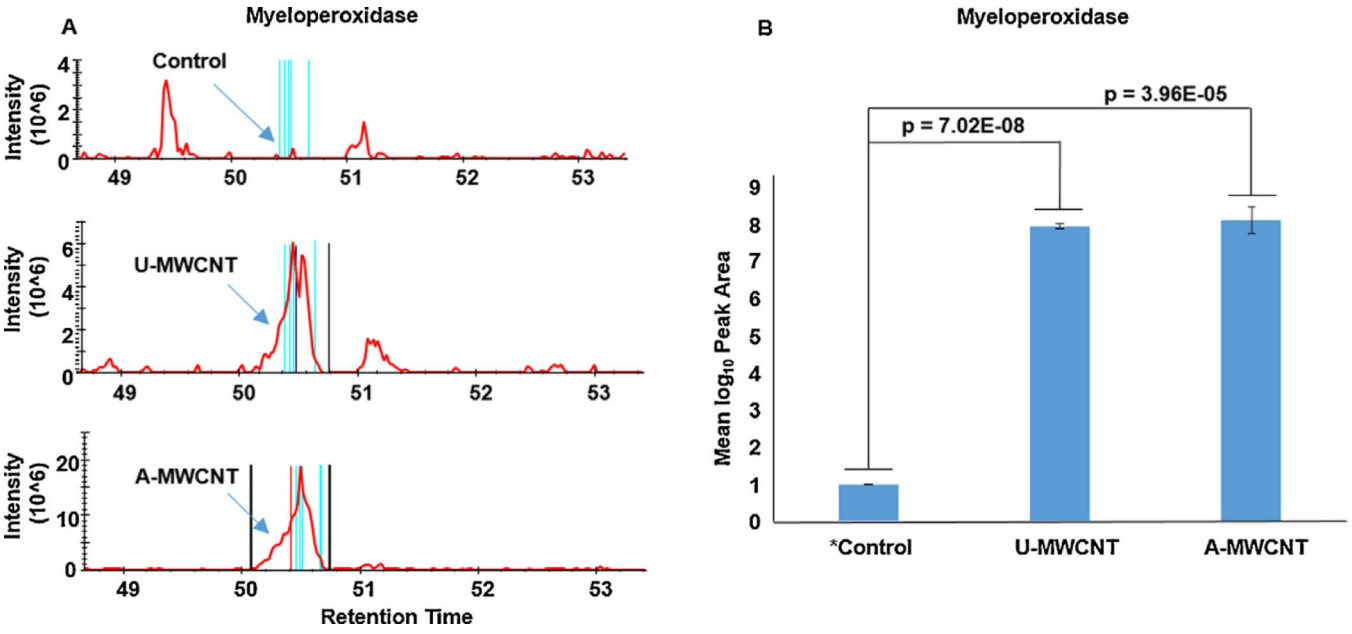

Fig. 4.

Peak area analysiswas conducted on proteins that were discovered to be significant using the Fisher's Exact test on the spectral count data. (A) Chromatogram overlay used to assess changes in peak area by group. (B) Peak area was tested for significance across every group using the two-sample *t*-test: Control versus U-MWCNT (p = 7.02E- 08), Control versus A-MWCNT (p = 3.96E-05), and U-MWCNT versus A-MWCNT = 0.679). *Control peak area = 0, but imputed as a value of 10 to allow for log adjustment. Peaks were identified using a combination of MS2 identification (blue lines), mass measurement accuracy (<3 ppm), dot products of theoretical isotope abundance, and retention time reproducibility (For interpretation of the references to colour in this figure legend, the reader is referred to the web version of this article.).

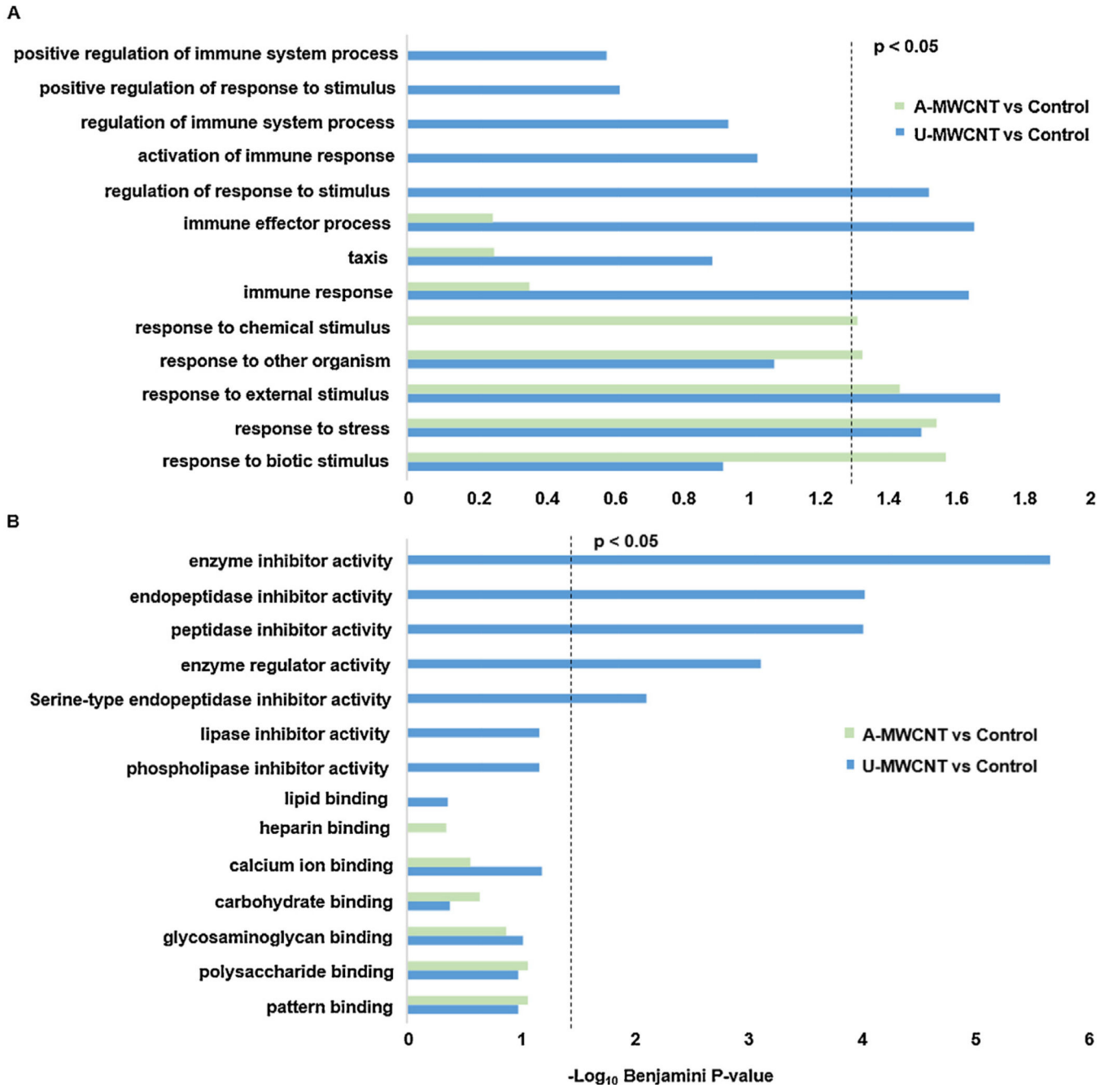

Fig. 5.

GO analysis terms for (A) Biological Process, and (B) Molecular Function for significant proteins by peak area analysis both of the exposed groups versus the control. Significance ($p<0.05$) was calculated by a modified Fisher's exact test (EASE score) and adjusted by the Benjamini correction and reported as the $-\log_{10}$ Benjamini p-value. Significant GO terms are illustrated to the right of the dashed line (Huang da et al., 2009).